Journal of Power Sources 195 (2010) 553–558

Contents lists available at ScienceDirect

Journal of Power Sources

journal homepage: www.elsevier.com/locate/jpowsour

Kinetic modeling of high pressure autothermal reforming

Mark A. Reese*, Scott Q. Turn[1], Hong Cui[2]

Hawaii Natural Energy Institute, University of Hawaii, 1680 East-West Rd., POST 109, Honolulu, HI 96822, United States

ARTICLE INFO

Article history:
Received 18 May 2009
Received in revised form 8 July 2009
Accepted 8 July 2009
Available online 23 July 2009

Keywords:
Kinetic modeling
Methane
Autothermal reforming
High pressure
Hydrogen production

ABSTRACT

Previously a lab scale catalytic autothermal reformer (ATR) capable of operating at pressures from 6 to 50 bar was constructed and tested. The objective of the experimental program was to maximize H_2 production per mole of O_2 supplied ($H_{2(out)}/O_{2(in)}$). In this companion paper a 1-D, heterogeneous, numerical model is developed and tested for simulating the high pressure ATR. The effects of molar steam to carbon (S/C) and oxygen to carbon (O_2/C) ratios are studied and optimal operating conditions are identified for three system operating pressures; 6, 28 and 50 bar. Experimental optimal conditions and model results are compared and found to be in close agreement. The optimal conditions, however, predicted by the model at pressures of 28 and 50 bar have higher S/C ratios and produce higher $H_{2(out)}/O_{2(in)}$ yields than the experimentally determined optimums. A sensitivity analysis consisting of 9 model parameters is also performed. The model is most sensitive to the activation energy of the two steam reforming reactions used in the model and the operating parameter O_2/C.

1. Introduction

Significant research and development effort has been expended to advance hydrogen as the energy carrier of tomorrow. While it is likely that future hydrogen will be produced from renewable resources such as biomass or electrolysis powered by geothermal, photovoltaic or wind, currently the most economic way to produce hydrogen is by catalytic thermochemical reforming of hydrocarbons. Methane in particular has been the primary source for hydrogen production and techniques developed for methane reforming can aid in transitioning to sustainable renewable sources of hydrogen for tomorrow. Over the last few decades, kinetic modeling of methane reforming through various thermochemical techniques has been reported in the literature. Results have identified methods to increase efficiency and provided insight useful in improving reactor design.

In light of advancing reforming techniques, there has been recent interest in constructing small scale, underwater, fuel reforming stations. Applications include powering underwater sensory equipment and recharging unmanned submersibles. In concept, these remote reforming stations, using onboard fuel cells to generate power, would be deployed on the ocean floor where near natural gas seeps or methane hydrates. Methane from these sources would be collected and purified to remove catalyst-poisoning H_2S and then reformed to produce a hydrogen rich gas for the fuel cell. While methane would be available in abundance, a major limitation for operating a reformer and fuel cell on the seafloor is having oxygen available at sufficiently high concentrations. Additionally, since the unit would be deployed on the ocean floor and operate at ambient pressure, design of components would need to accommodate the effects of elevated pressure on the physical system and reformer and fuel cell chemistry. An alternative to operating the reformer at ambient pressure would be to operate the reformer in a submerged pressure hull that would allow the system to operate at a lower pressure. The latter system would require that methane at the ambient pressure of the ocean floor be decompressed and that unwanted byproducts be recompressed for removal from the pressure hull. Operating the reformer at ambient pressure was selected over this alternative. For this fuel-rich, oxygen limited, reforming application it is of particular interest to maximize moles of H_2 produced per mole of O_2 supplied.

Results of an experimental, laboratory-investigation of methane reforming at simulated sea floor pressure conditions were reported in a previous paper by the same authors [1]. This paper reports a companion modeling effort that explores elevated pressure reforming via numerical simulation.

1.1. Modeling

This section briefly describes modeling work which has been conducted on the three main thermochemical catalytic reforming techniques; steam reforming (SR), partial oxidation reforming (POX) and autothermal reforming (ATR). It should be noted at the

* Corresponding author. Tel.: +1 808 956 5397; fax: +1 808 956 2344.
E-mail addresses: mareese@hawaii.edu (M.A. Reese), sturn@hawaii.edu (S.Q. Turn), hongcui@hawaii.edu (H. Cui).
[1] Tel.: +1 808 956 2346; fax: +1 808 956 2336.
[2] Tel.: +1 808 956 5397; fax: +1 808 956 2344.

0378-7753/$ – see front matter © 2009 Elsevier B.V. All rights reserved.
doi:10.1016/j.jpowsour.2009.07.031

Nomenclature

C_i	concentration of gas species i (mol m^{-3})
C_i^{in}	concentration of inlet gas species i (mol m^{-3})
$\overline{c_{pg}}$	average specific heat of gas (J kg^{-1} K^{-1})
d_p	catalyst pellet diameter (m)
D_{dpi}	dispersion coefficient of gas species i
D_i	gas diffusivity of species i (m^2 s^{-1})
h	heat transfer coefficient between catalyst bed and gas phase (W m^{-3} K^{-1})
i	species index
j	reaction index
ΔH_j	heat of reaction j (J mol^{-1})
m_{ave}	average molar mass of gas into which gas species i is diffusing (g mol^{-1})
m_i	mass of gas species i (g mol^{-1})
P	system pressure (bar)
p_i	partial pressure of gas species i (bar)
r_i	reaction rate of gas species i (mol kg^{-1} catalyst s^{-1})
R_j	reaction rate of reaction j (mol kg^{-1} catalyst s^{-1})
S_h	heat transfer area per unit volume of catalyst bed (m^{-2} m^{-3})
t	time (s)
T	temperature of gas phase (K)
T^{in}	gas inlet temperature (K)
T_s	temperature of solid phase (K)
u	superficial gas velocity (m s^{-1})
z	coordinate (m)

Greek symbols

ε	void fraction of the catalyst bed
λ	effective thermal conductivity of catalyst bed (W m^{-1} K^{-1})
ρ_{cat}	density of catalyst bed (kg catalyst m^{-3})
$\overline{\rho_g}$	average gas density (kg m^{-3})
τ_{bed}	tortuosity of the bed

Subscripts

bed	catalyst bed
cat	catalyst
g	gas
i	gas species (H_2, O_2, CO, CO_2, H_2O, CH_4)
j	reaction index (1–4)

outset that SR and POX have been implemented in industry for some time [2]. As such, much literature can be found describing the thermodynamics and kinetics of relevant reactions. In comparison, relatively few papers exist on the kinetics of ATR. The following is a brief sample of thermochemical reforming models which have been developed and studied.

1.2. Steam reforming

In 1989, Xu and Froment developed a rate equation and kinetic data for methane steam reforming (MSR) [3]. Their study was conducted in the temperature range of 573–823 K with gauge pressure varying from 0.3 to 10 bar. A conventional tube reactor was used and Ni based catalyst employed. Their work formed a basis for much modeling work in the MSR field and has also carried over into POX and ATR work. Hou and Hughes [4] developed slightly different rate equations and kinetic data and tested their model at 1.2–3.0 bar. Both SR models consisted of three global reactions: two endothermic steam reforming reactions:

$$CH_4 + H_2O \rightarrow CO + 3H_2, \qquad \Delta H_{1(298)} = 206\ \text{kJ mol}^{-1} \tag{1}$$

$$CH_4 + 2H_2O \rightarrow CO_2 + 4H_2, \qquad \Delta H_{2(298)} = 165\ \text{kJ mol}^{-1} \tag{2}$$

and the exothermic water gas shift reaction:

$$CO + H_2O \rightarrow CO_2 + H_2, \qquad \Delta H_{3(298)} = -41\ \text{kJ mol}^{-1} \tag{3}$$

1.3. Partial oxidation reforming

Modeling of POX was outlined by De Groote and Froment in 1996 [5]. Their model was based on the use of a Ni catalyst and consisted of rate expressions for nine reactions including Eqs. (1)–(3) and an additional six reactions describing methane combustion, CO_2 reforming, carbon deposition, methane cracking, and carbon oxidation. The reaction set was employed in a one-dimensional, fixed bed, adiabatic, heterogeneous model based on work from Froment and Bishoff [6].

Other models, such as the POX membrane reactor proposed by Basile et al. in 2001 [7], used only reactions in Eqs. (1)–(3) and the combustion of methane:

$$CH_4 + 2O_2 \rightarrow CO_2 + 2H_2O, \qquad \Delta H_{4(298)} = -802\ \text{kJ mol}^{-1} \tag{4}$$

Like many, the model proposed by Basile et al. was one-dimensional and valid near atmospheric pressure (1.2 bar)

1.4. Autothermal reforming

Chan and Wang [8] provided an overview of ATR performance using chemical equilibrium models and identified operating conditions to maximize H_2 yield while minimizing CO production and avoiding carbon deposition. To further the research in this field, Hoang and Chan described ATR kinetics in 2004 [9]. This would be the first of their series of papers on kinetic modeling of MSR, POX and ATR [10–12]. Their reaction scheme for ATR was a combination of SR, based on Xu and Froment [3], and POX reforming reactions. Including only those reactions with significant rates [12] led to a reduced reaction set based on Eqs. (1)–(4). All reforming papers by Hoang et al. used a two-dimensional, heterogeneous model at atmospheric pressure.

In 2006, Lee et al. [13] presented results from a one-dimensional, pseudo-homogenous model based on Hoang and Chan's reaction scheme. The effects of steam to carbon (S/C) and oxygen to carbon (O_2/C) molar ratios in the reactant streams to the reformer were studied at atmospheric pressure.

De Groote and Froment reported simulating a 25 bar ATR condition while validating their POX model, but this was only a single run and no study involving pressure effects was presented [5].

In 1998, Olsvik and Hansen presented a paper on high pressure autothermal reforming. Their work, however, dealt primarily with fluid flow, combustion kinetics, and soot formation. No data on product gas composition for the various reformer conditions of interest were presented [14].

Therefore, while many papers dealing with thermodynamics and kinetics of various reforming techniques exist, very few papers have been found which deal with high pressure methane ATR.

1.5. Objectives

The objectives of this study were to adopt a suitable model for high pressure ATR in order to compare modeling results with experimental results previously reported [1] and to conduct a sensitivity analysis of the model.

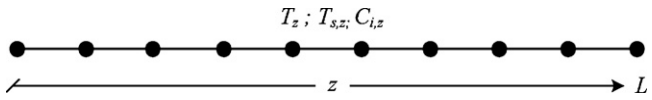

Fig. 1. Schematic layout of 1-D reactor.

2. Materials and methods

A one-dimensional ATR model based on mass, energy, and species balances was developed which included kinetic rate expressions for chemical reactions. The model was solved using the software package, COMSOL Multiphysics 3.4 (COMSOL, Inc., Los Angeles, CA) based on the finite element method (FEM).

2.1. Model description

The model was based on reactions in Eqs. (1)–(4) and included seven gas species: methane, oxygen, steam, carbon monoxide, carbon dioxide, hydrogen, and nitrogen. A schematic layout of the 1-D reactor model is shown in Fig. 1. T_z represents the gas phase temperature, $T_{s,z}$ represents the solid phase temperature, and $C_{i,z}$ represents the concentration of gas species i at a given location z. L represents the length of the catalyst bed (0.61 m) and the nodes at which the solution is calculated are represented by dots.

2.2. Model assumptions

Model development included the following assumptions: (1) convective transport dominates diffusive transport in the axial direction for thermal and mass diffusion (Péclet number ≥140 and ≥40, respectively) allowing the diffusion terms to be omitted, (2) the thermal conductivity of the gas phase is much smaller than that of the solid phase catalyst bed and can be omitted, (3) radial variations are considered negligible and therefore all radial components are omitted.

2.3. Model equations

The kinetic rate equations and kinetic parameters, equilibrium constants and adsorption constants were obtained from a publication by Hoang et al. that employed Engelhard's Ni-0309S catalyst [11]. With the assumptions mentioned above the three governing equations that describe the model are listed below. Eqs. (5)–(7) are the gas phase species balance, the energy balance for the solid phase, and the energy balance for the gas phase, respectively.

$$\varepsilon\frac{\partial C_i}{\partial t} = -u\frac{\partial C_i}{\partial z} + \rho_{cat} r_i, \quad i = 1 \text{ to number of species} \tag{5}$$

$$\rho_b c_{pcat}\frac{\partial T_s}{\partial t} = \lambda\frac{\partial^2 T_s}{\partial z^2} + \rho_{cat}\sum_{j=1}^{4}(-\Delta H_j)R_j + S_h h(T - T_s) \tag{6}$$

$$\varepsilon\overline{\rho_g c_{pg}}\frac{\partial T}{\partial t} = -u\overline{\rho_g c_{pg}}\frac{\partial T}{\partial z} + S_h h(T_s - T) \tag{7}$$

where

$$D_{dpi} = \varepsilon\left(\frac{D_i}{\tau_{bed}} + 0.5 d_p u\right) \tag{8}$$

and

$$\tau_{bed} = \frac{1}{\sqrt{\varepsilon}} \tag{9}$$

$$D_i = 1\times 10^6 \cdot T^{1.75} \cdot \frac{((1/m_{ave}) + (1/m_i))^{1/2}}{P((20.1)^{1/3} + (p_i * 20.1)^{1/3})^2} \tag{10}$$

2.4. Boundary conditions

The following boundary conditions were specified in the model:

at the reactor inlet, $z = 0$ $\quad T = T^{in}; T_s = T^{in}; C_i = C_i^{in}$ (11)

and at the reactor outlet, $z = L$ $\quad \frac{\partial T}{\partial z} = 0; \lambda\frac{\partial T_s}{\partial z} = 0; \frac{\partial C_i}{\partial z} = 0$ (12)

2.5. Initial conditions

The model was initialized with the following values. The inlet temperature of the gas species, T^{in}, was set to the experimental inlet temperature of 270 °C [1]. The catalyst bed temperature was given a linear profile from 270 °C at the reactor inlet to 700 °C at the reactor outlet. The CH_4 flow rate (2.5 l min^{-1}), N_2 flow rate (0.5 l min^{-1}), appropriate steam to carbon (S/C) and oxygen to carbon (O_2/C) (variable) ratios and pressure (6, 28, or 50 bar) were also specified. While the inlet temperature and gas flow rates were held at their initial values over the course of a run, the catalyst bed temperature profile was not and the profile changed significantly as the reactions occurred.

2.6. Solver and mesh size

A time dependent solver was used to propagate the model solution from the initial conditions. Using the temperature profile assigned to the catalyst bed the reaction started at the outlet of the reactor and propagated toward the inlet, until the reaction zone stabilized. The results from this apparent steady state solution determined with the time dependent solver were saved and used as the initial conditions for the stationary solver. This was done to verify the time dependent solution. If the results converged using the stationary solver, a steady state solution for the set of operating condition was assumed to have been reached. A parametric solver was subsequently used to determine solutions for different values of model parameters.

The mesh size was critical to ensure accurate results from the model. If the mesh was too large, steep gradients were missed and faulty calculations made. Mesh refinement was performed to determine if the mesh size in use was small enough.

3. Results and discussion

3.1. Comparison of modeling and experimental results

The results of the ATR model were compared to the experimental results previously acquired [1]. The experimental optimal condition for maximizing $H_{2(out)}/O_{2(in)}$ at 6 bar (O_2/C = 0.44; S/C = 3.35), 28 bar (O_2/C = 0.48; S/C = 3.0) and 50 bar (O_2/C = 0.48; S/C = 3.0) for experimental and model output gas composition is compared on the parity plot shown in Fig. 2. All data points are moles of gas species out divided by moles of gas species in unless otherwise noted. Under these conditions, experimentally, one mole of O_2 produced 4.16, 3.43 and 2.84 moles of H_2 at 6, 28 and 50 bar, respectively. The models' correlation to experimental results for these conditions is high. In fact the model was able to predict the decreased performance at increased pressure very well: all predicted results were within ±10% of experimental results except the moles of $CO_{(out)}/CH_{4(in)}$. It should be noted that Boudouard's equation was not included in the model and therefore the model is not suitable for predicting carbon formation. This approach was taken since the operating conditions tested in previous experimental work [1] did not favor carbon formation.

Since the model predicted outlet gas composition in high correlation to the experimental results, the model was used to look at a broader range of operating conditions than experimentally tested.

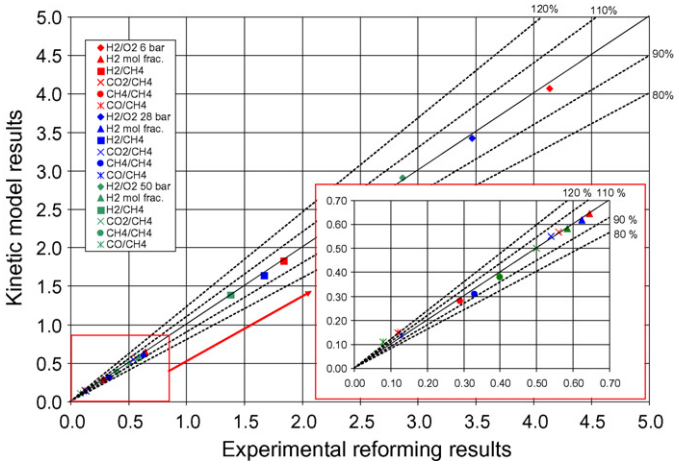

Fig. 2. Parity plot of experimental results and kinetic model results at 6, 28 and 50 bar. (All data points are moles of gas species out divided by moles of gas species in unless otherwise noted.)

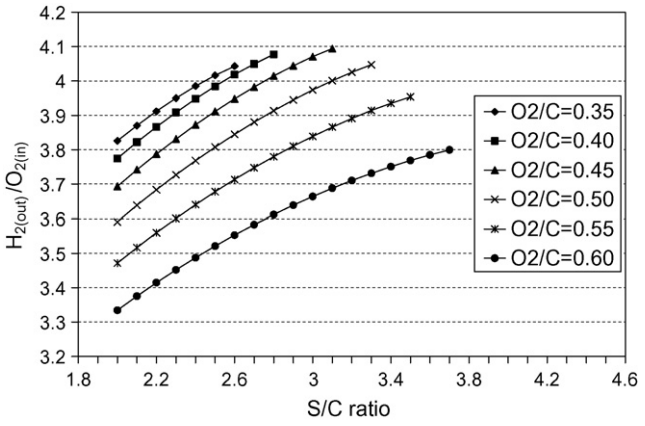

Fig. 3. Moles of $H_{2(out)}/O_{2(in)}$ model results for 6 bar (various O_2/C and S/C ratios).

Figs. 3–5 show the moles $H_{2(out)}/O_{2(in)}$ over the full range of conditions modeled for 6, 28, and 50 bar, respectively. Only moles of $H_{2(out)}/O_{2(in)}$ is shown since this was the focus of the accompanying experimental work.

The experimental work identified reformer operating points that were not stable and resulted in the high temperature reaction zone being blown out of the reactor. This behavior was observed in the model results as well. For a fixed pressure and O_2/C ratio the

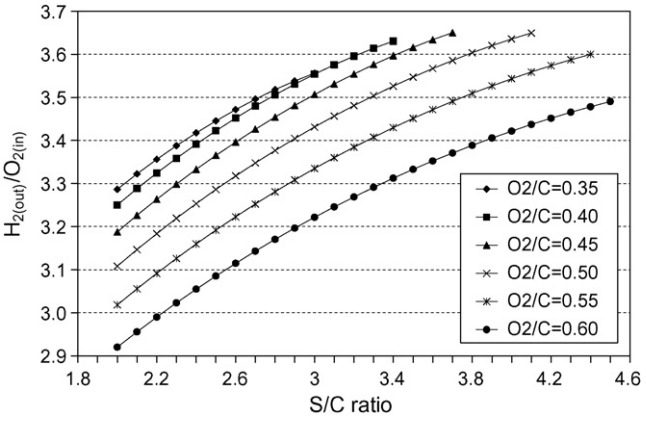

Fig. 4. Moles of $H_{2(out)}/O_{2(in)}$ model results for 28 bar (various O_2/C and S/C ratios).

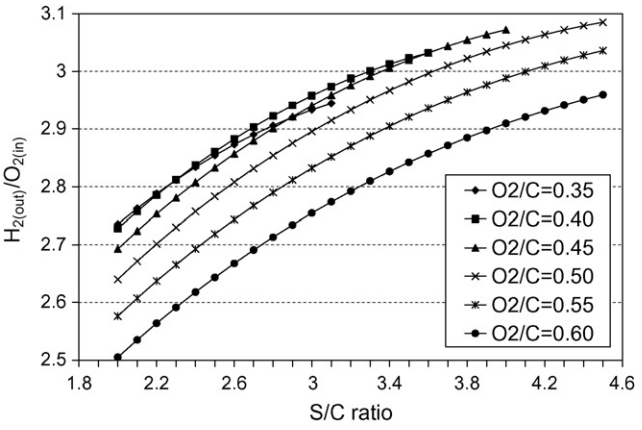

Fig. 5. Moles of $H_{2(out)}/O_{2(in)}$ model results for 50 bar (various O_2/C and S/C ratios).

model would attempt to parametrically solve a series of different S/C ratio's. With a starting value of 2.0 the S/C ratio would be gradually increased with a small step size to a final value of 4.5. In nearly every test, however, at a particular S/C ratio, the high temperature reaction zone would move downstream through the reactor with large steps when the S/C ratio was increased ever so slightly. When this occurred, modeling for the given O_2/C ratio was stopped and then restarted using the next O_2/C ratio to be tested with a S/C value of 2.0. For example in Fig. 3 at an O_2/C ratio of 0.35 when the S/C ratio reached 2.6 this phenomenon was observed. At that point modeling was restarted at an O_2/C ratio of 0.40 and a S/C ratio of 2.0.

It was observed that as pressure increased a higher S/C ratio was attainable for a given O_2/C ratio. This was due to both the higher resulting reactor temperature and the lower resulting space velocity which helped keep the flame front from blowing out the back end of the reactor.

The optimal yield and operating condition for moles of $H_{2(out)}/O_{2(in)}$ predicted by the model was 4.09 at 6 bar (O_2/C = 0.45; S/C = 3.1), 3.65 at 28 bar (O_2/C = 0.5; S/C = 3.7) and 3.08 at 50 bar (O_2/C = 0.50; S/C = 4.4). At 6 bar the predicted optimum and the corresponding O_2/C and S/C ratios are very comparable to the experimental values. At 28 and 50 bar the predicted optimum was higher and also occurred at a higher S/C but comparable O_2/C ratio when compared to experimental values. This suggests that the model was able to run under conditions having greater S/C ratios than experimentally observed at elevated pressures. Being able to run with a higher S/C ratio meant higher molar $H_{2(out)}/O_{2(in)}$ yield's were attainable.

Fig. 6 shows the predicted moles of $H_2/O_{2(in)}$ along the length of the reactor at various S/C ratios an O_2/C ratio of 0.5 and a pressure of 50 bar. The model predicted a very steep increase in moles of $H_2/O_{2(in)}$ near the inlet with a much more gradual increase towards the backend of the reactor. The slope of the moles of $H_2/O_{2(in)}$ curve at the front of the reactor is determined by two factors: the cooling effect of steam which is injected at 270 °C and the space velocity which increased with increasing S/C ratios. Therefore, with each increase in the S/C ratio the moles of $H_2/O_{2(in)}$ curve became more gradual at the front of the reactor in spite of reaching higher final values. The most extreme example is observed at a S/C ratio of 4.5 where the curve is clearly pushed downstream. Also note, although pressure effects are not shown in Fig. 6, the difference in the $H_2/O_{2(in)}$ yield between successive S/C ratios decreased as pressure increased. This suggests the model is more sensitive to the S/C ratio at low pressures than it is at elevated pressures.

Figs. 7–9 shows the dry percent volume of each species in the reformate gas over a range of S/C ratios at an O_2/C ratio of 0.5 and

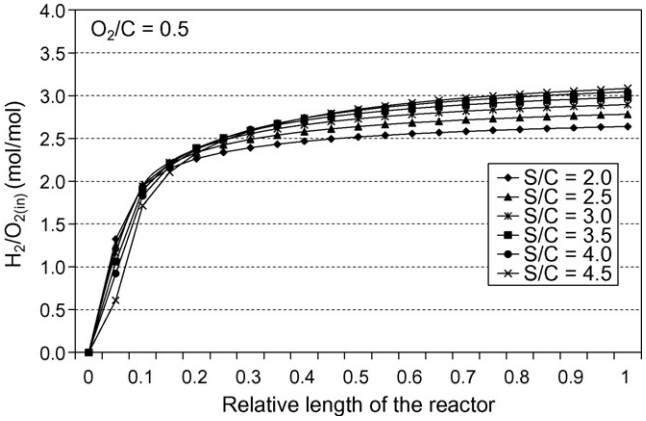

Fig. 6. Moles of $H_2/O_{2(in)}$ model results for 50 bar along the reactor length (various S/C ratios).

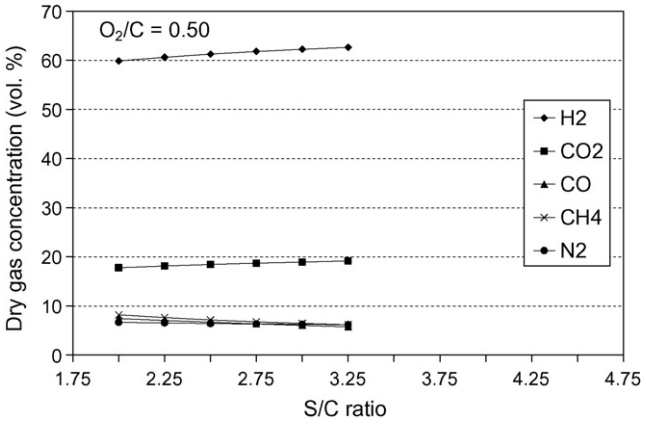

Fig. 7. Kinetic model results: dry gas concentration (various S/C; $O_2/C = 0.5$; 6 bar).

pressures of 6, 28 and 50 bar. The trends at each pressure are the same: an increased S/C ratio led to increased percentages of H_2 and CO_2 and corresponding decreases in CH_4, CO, and N_2. As pressure increased, however, the percentages of CO and CO_2 remained nearly identical while the concentrations of CH_4 and N_2 increased and H_2 decreased.

3.2. Sensitivity analysis

Figs. 10 and 11 illustrate the sensitivity of the kinetic model with respect to 9 model parameters: the steam to carbon ratio (S/C), oxygen to carbon ratio (O_2/C), reaction rate of reaction 1 (RR1), reaction rate of reaction 2 (RR2), activation energy of reaction 1 (E1), activation energy of reaction 2 (E2), overall heat loss (HL), conductivity of the catalyst bed (Cat k), and pressure (P). The reaction rate and activation energy of reaction 3 and 4 had a negligible effect in all studies and therefore were not presented. Five different model outputs (moles of H_2, CO, CO_2, CH_4, and % H_2) were studied by varying the 9 model parameters ±25% from their standard value when run at 28 bar a S/C = 3.0 and an $O_2/C = 0.48$.

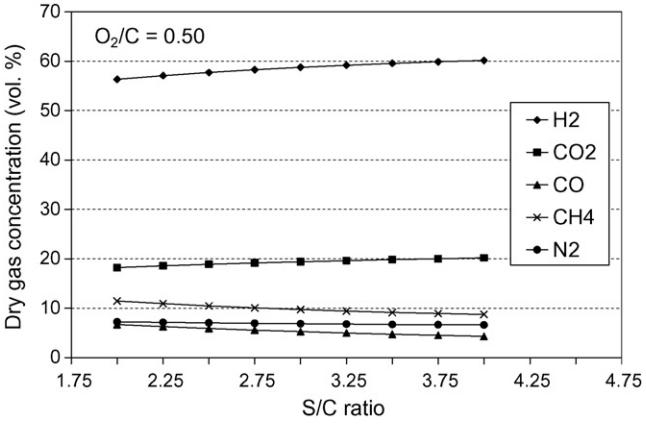

Fig. 8. Kinetic model results: dry gas concentration (various S/C; $O_2/C = 0.5$; 28 bar).

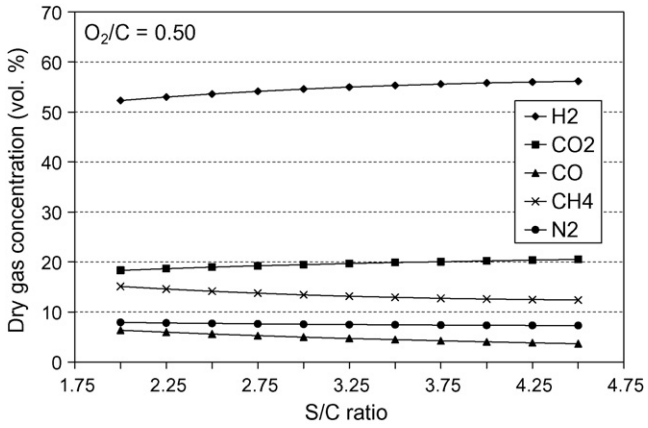

Fig. 9. Kinetic model results: dry gas concentration (various S/C; $O_2/C = 0.5$; 50 bar).

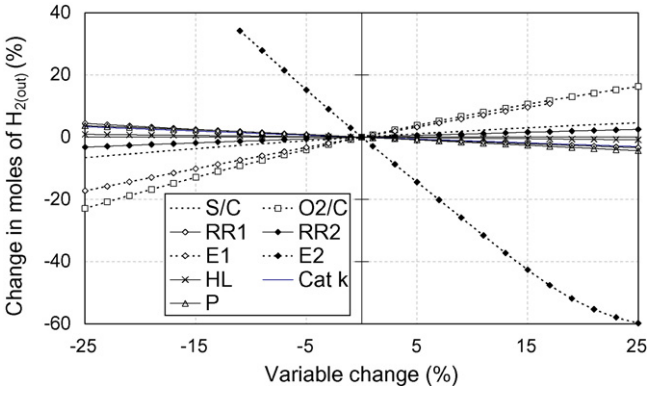

Fig. 10. Moles of $H_{2(out)}$ sensitivity analysis (28 bar).

The moles of $H_{2(out)}$ was most sensitive to E2 followed by O_2/C and E1. A 25% increase in E2 and O_2/C resulted in a 60% decrease and >15% increase in moles of $H_{2(out)}$, respectively. Similarly a 25% decrease in RR1 decreased the moles of $H_{2(out)}$ by over 15%. The

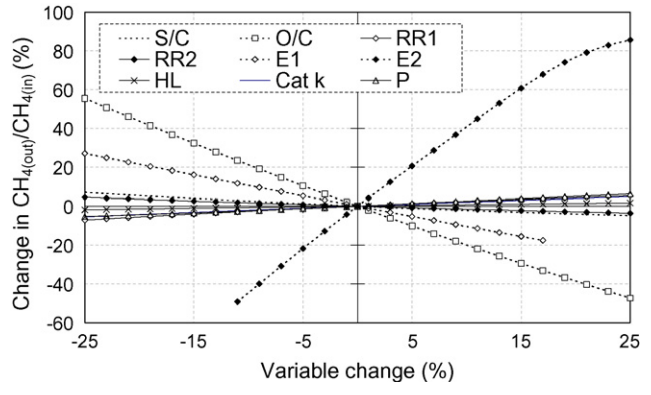

Fig. 11. Moles of $CH_{4(out)}$ sensitivity analysis (28 bar).

sensitivity analysis of the % $H_{2(out)}$ as well as the moles of $CO_{(out)}$ and $CO_{2(out)}$ followed the same trend as $H_{2(out)}$. The trends in the sensitivity analysis for the moles of $CH_{4(out)}$ were nearly the opposite of the $H_{2(out)}$ trends and can be seen in Fig. 11.

The moles of $CH_{4(out)}$ was most sensitive to E2 and O_2/C followed by E1. By increasing E2 25% the moles of $CH_{4(out)}$ increased by over 80%, by increasing O_2/C 25% the moles of $CH_{4(out)}$ decreased by over 40% and finally by decreasing E1 25% the moles of $CH_{4(out)}$ decreased by nearly 30%.

In summary the model output parameters were most sensitive to E2, O_2/C, and E1, respectively. In all cases, increasing E2 had the opposite effect of increasing E1 and O_2/C. Therefore increasing E2, or decreasing E1 and O_2/C, resulted in an increase in the moles of $CH_{4(out)}$ and a decrease in the moles of $H_{2(out)}$, $CO_{(out)}$, and $CO_{2(out)}$ and % $H_{2(out)}$. The model tended to be the least sensitive to HL and RR2.

4. Conclusions

A 1-D, heterogeneous, kinetic model was adapted for high pressure ATR and tested. Experimental optimal conditions and model results at 6, 28 and 50 bar were compared and found to be in close agreement. At elevated pressures the model predicted stable reformer operation at S/C ratios higher than were experimentally possible for a given O_2/C ratio. Optimal conditions predicted by the model at pressures of 28 and 50 bar had higher S/C ratios and produced higher $H_{2(out)}/O_{2(in)}$ yields than the experimentally determined optimums. The optimum conditions predicted by the model at 6 bar was 4.09 moles of $H_{2(out)}/O_{2(in)}$ (O_2/C = 0.45; S/C = 3.1), at 28 bar was 3.65 moles of $H_{2(out)}/O_{2(in)}$ (O_2/C = 0.5; S/C = 3.7) and at 50 bar was 3.08 moles of $H_{2(out)}/O_{2(in)}$ (O_2/C = 0.50; S/C = 4.4). A sensitivity analysis performed on the model showed that the model was most sensitive to the activation energy of the two steam reforming reactions used in the model and the operating parameter O_2/C. By using modeling techniques the effects of individual system variables on system performance were studied and optimal operating conditions were identified for three system operating pressures.

Acknowledgement

This work was supported by the Office of Naval Research under contract number N00014-06-0086.

References

[1] M.A. Reese, S.Q. Turn, H. Cui, J. Power Sources 187 (2) (2009) 544–554.
[2] J. Larmine, A. Dicks, Fuel Cell Systems Explained, 2nd ed., John Wiley and Sons Ltd., West Sussex, 2005, p. 406.
[3] G.F.F. Jianguo Xu, AIChE J. 35 (1) (1989) 88–96.
[4] K. Hou, R. Hughes, Chem. Eng. J. (Lausanne) 82 (1–3) (2001) 311–328.
[5] A.M. De Groote, G.F. Froment, Appl. Catal. A: Gen. 138 (2) (1996) 245–264.
[6] G.F. Froment, K.B. Bishoff, Chemical Reactor Analysis and Design, 2nd ed., 1990, p. 662.
[7] A. Basile, L. Paturzo, F. Lagana, Catal. Today 67 (1–3) (2001) 65–75.
[8] S.H. Chan, H.M. Wang, Int. J. Hydrogen Energy 25 (5) (2000) 441–449.
[9] D.L. Hoang, S.H. Chan, Appl. Catal. A: Gen. 268 (1–2) (2004) 207–216.
[10] D.L. Hoang, S.H. Chan, O.L. Ding, Chem. Eng. Res. Des. 83 (A2) (2005) 177–186.
[11] D.L. Hoang, S.H. Chan, O.L. Ding, J. Power Sources 159 (2) (2006) 1248–1257.
[12] D.L. Hoang, S.H. Chan, O.L. Ding, Chem. Eng. J. (Amsterdam, Netherlands) 112 (1–3) (2005) 1–11.
[13] S. Lee, J. Bae, S. Lim, Proceedings of the International Conference on Fuel Cell Science, Engineering, and Technology, 4th, Pt. B, Irvine, CA, United States, June 19–21, 2006, pp. 647–652.
[14] O. Olsvik, R. Hansen, Stud. Surf. Sci. Catal. 119 (Natural Gas Conversion V) (1998) 875–882.